Spectrally bright and broad fiber-based heralded single-photon source

E. A. Goldschmidt, M. D. Eisaman, J. Fan,* S. V. Polyakov, and A. Migdall
Optical Technology Division, National Institute of Standards and Technology, Gaithersburg, Maryland 20899, USA
and Joint Quantum Institute, University of Maryland, College Park, Maryland 20742, USA
(Received 18 March 2008; published 29 July 2008)

We present an experimental characterization of a heralded single-photon source based on spontaneous four-wave mixing in a single-mode microstructure fiber. We measure the second-order correlation function $g^{(2)}(0)$ to be far below the classical, Poissonian limit of 1 over a broad spectral range. With single-spatial-mode output, such a spectrally bright and broad fiber-based heralded single-photon source is suitable for a variety of quantum-information applications.

DOI: 10.1103/PhysRevA.78.013844 PACS number(s): 42.50.Ar, 42.65.−k

A reliable source of single photons in well-defined spatial and temporal modes is an essential element for a number of quantum computation and quantum key distribution protocols [1–3]. Single-photon sources can be divided broadly into two categories: on-demand sources whose operation is ideally deterministic, and heralded sources, which are inherently probabilistic. On-demand sources deterministically emit a single photon at a time specified by the user, and include sources based on semiconductor quantum dots [4], mesoscopic quantum wells [5], molecules [6], single atoms in cavities [7], single ions [8], atomic ensembles [9], and nitrogen-vacancy centers in diamond [10]. Heralded single-photon sources are based on the probabilistic emission of correlated photon pairs, and herald the presence of one photon by the detection of the second photon of a pair. Heralded single-photon sources have traditionally been based on spontaneous parametric down-conversion (PDC) in a bulk crystal [11,12] or a crystal waveguide [13], although other approaches have been pursued such as atomic cascades [14]. Significant progress has been made toward solving the technical challenge of efficiently coupling single photons from a bulk crystal into a single-spatial-mode optical fiber [15].

Recent experiments have shown that the nonlinear wavelength conversion efficiency possible with spontaneous four-wave mixing (FWM) in single-mode optical fibers [16–18] is similar to the efficiency of PDC in bulk crystals or waveguides. FWM in optical fibers produces correlated photon pairs with high two-photon spectral brightness over a broad spectral range in a single spatial mode [17]. These features give fiber-based sources of correlated photon pairs unique advantages as heralded single-photon sources; for example, the broad spectral bandwidth possible with four-wave mixing in optical fibers allows wavelength division multiplexing at the single-photon level, and the single-spatial-mode output allows photon collection with high efficiency. In this paper, we present an experimental characterization of a fiber-based heralded single-photon source. We have measured the conditional second-order correlation function [19] $g^{(2)}(0)$ of the heralded single photons to be much less than unity over a broad spectral range, suggesting that fiber-based heralded single-photon sources is suitable for future quantum-information applications.

*Jfan@nist.gov

In the experiment (Fig. 1), 8 ps pulses from a Ti:sapphire laser are coupled into a microstructure fiber at a repetition rate of 76 MHz, with wavelength ($\lambda_{\text{pump}}=740.6$ nm) located slightly on the normal-dispersion side of the fiber (zero-dispersion wavelength $\lambda_{\text{ZDW}}=745\pm5$ nm). The high third-order nonlinearity ($\gamma=70\ \text{W}^{-1}\ \text{km}^{-1}$) of the fiber and careful selection of phase-matching conditions enables efficient two-photon generation via FWM that is outside the primary Raman-scattering spectral band (peaked at 765 nm; see Fig. 2 inset). With this particular pumping configuration, we measured a 20-nm-wide bandwidth where the FWM signal is large but the accidental two-photon coincidence noise is small [17]. A two-pass grating configuration is adopted to select the frequency-conjugated signal (λ_s) and idler (λ_i) photon wavelengths that are connected by energy conservation, $2\omega_{\text{pump}}=\omega_s+\omega_i$. A slit in the signal (idler) path allows selection of the signal (idler) wavelength via the position of the slit and the signal (idler) bandwidth via the width of the slit. Because the FWM process creates correlated pairs of signal and idler photons, the detection of a signal photon can be used to herald the existence of an idler photon, or vice versa.

The quantum state for photon pairs emitted via FWM in an optical fiber can be approximately described as

$$\psi \sim \sqrt{p(0)}|0_s0_i\rangle + \sqrt{p(1)}|1_s1_i\rangle + \sqrt{p(2)}|2_s2_i\rangle + (\text{higher-order processes}), \quad (1)$$

where $|\alpha_s\beta_i\rangle$ denotes the state with α signal photons and β idler photons, and $p(n)$ represents the probability of producing n signal-idler photon pairs. Equation (1) also holds for the emission of correlated photon pairs in PDC-type sources. (Here we drop the spatial, temporal, or polarization mode for simplicity.) When operating with a small *mean photon number*, the quantum state appears mostly in the vacuum state $[p(0)\sim1]$, with a small probability $[p(1)\ll1]$ to create one correlated photon pair and an even smaller probability $[p(2)\sim p^2(1)]$ to have two photon pairs created one at a time. While the gain of PDC linearly depends on the pump power P, with $p(1)\sim P$ and $p(2)\sim P^2$, the gain of FWM has a quadratic dependence on P, with $p(1)\sim P^2$ and $p(2)\sim P^4$. In both cases, the emission of multiple photon pairs can become significant with increased pump power. The emission of multiple photon pairs is harmful to quantum-information appli-

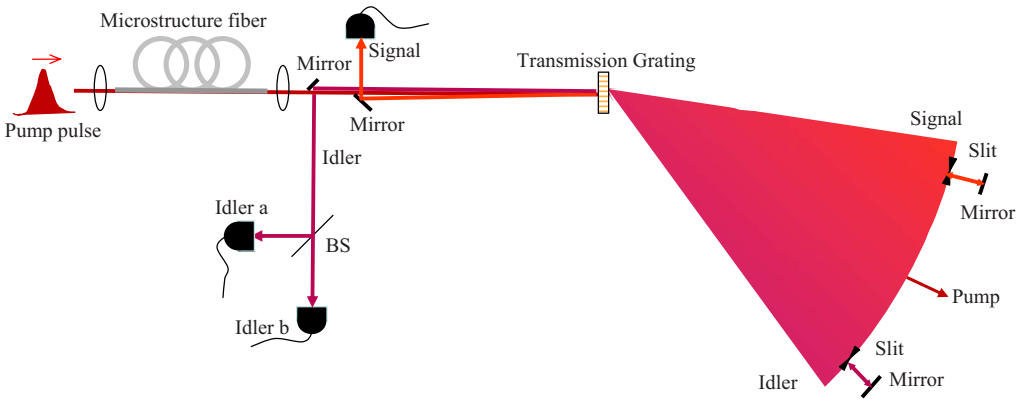

FIG. 1. (Color online) Experimental setup. BS: 50:50 beam splitter.

cations because it allows eavesdropping (when one is trying to generate heralded single photons) or decreases the visibility (when one is trying to generate entangled photon pairs) [1]. The higher-order processes can be effectively suppressed when the *mean photon number* is small. The influence of multiple-photon-pair-emission processes can be characterized using the second-order correlation function $g^{(2)}(0)$. To measure $g^{(2)}(0)$ in our experiment we insert a non-polarizing beam splitter in the idler path (see Fig. 1). Conditional on the detection of a signal photon, the $g^{(2)}(0)$ of the idler field is defined as [19]

$$g^{(2)}(0) = \frac{\langle :\hat{n}_a \hat{n}_b: \rangle}{\langle \hat{n}_a \rangle \langle \hat{n}_b \rangle}, \tag{2}$$

where $\hat{n}_a$ and $\hat{n}_b$ denote the photon-number operators (evaluated at identical times) for the two idler detectors (see Fig. 1) and : : denotes operator normal ordering. It is easy to see that for small mean photon number we have

$$g^{(2)}(0) = \frac{p_{ab}(2)}{p_a(1)p_b(1)} \approx \frac{2p(2)}{p^2(1)}, \tag{3}$$

where $p_a(1) \approx \eta_a p(1)/2$ and $p_b(1) \approx \eta_b p(1)/2$ denote the probabilities of detecting one photon at idler detectors a and b, respectively, and $p_{ab}(2) \approx \eta_a \eta_b p(2)/2$ denotes the joint probability of simultaneously detecting one photon at idler detector a and one photon at idler detector b. The overall single-photon detection efficiencies are $\eta_s = 5\%$ for the signal arm, and $\eta_a = 7\%$ ($\eta_b = 7\%$) for idler arm a (idler arm b). [Breakdown of signal (idler) photon detection efficiencies: quantum efficiency of single-photon avalanche photodiode (APD)=60% (50%), fiber coupling efficiency=53% (58%), interference filter transmittance=53% (60%), two passes through transmission grating efficiency=39% (58%), efficiency from other optics=75% (70%).]

For a perfect single-photon source and a perfect single-photon detector (with zero dark counts), the numerator in Eq. (2) is always zero since detectors a and b never simultaneously detect a photon, and therefore $g^{(2)}(0)$ equals zero. For any source with a nonzero probability of multiple-photon-pair emission we can see that $g^{(2)}(0) > 0$. A semiclassical theory of light predicts a lower limit of 1 on $g^{(2)}(0)$, and thus $g^{(2)}(0) < 1$ signifies the nonclassical nature of the field being measured [20]. In addition, it can be shown that $g^{(2)}(0) = 1$ for a source with Poissonian statistics, such as a coherent laser, and $g^{(2)}(0) = 2$ for a source with thermal statistics, such as spontaneous Raman scattering [20,21]. We want to emphasize that the measurement of $g^{(2)}(0)$ presented in this paper also provides an important reference to the development of fiber-based sources of entangled photon pairs. The observed decreasing ratio of two-photon coincidence rate to accidental coincidence rate for increasing pump power is partially due to the increased emission probability of multiple photon pairs [17].

In the experiment, photons collected in the signal and two idler arms are independently coupled into a four-channel silicon APD array. Each APD functions independently, outputting an electrical signal when detecting a photon. The electrical signals are fed into a home-built field-programmable gate array (FPGA) that is synchronized to the 76 MHz pulsed laser and has 13-ns-wide time bins [22]. The FPGA compares the input signals and reports coincidence analysis to a data-taking computer. Relative delays between signals from different channels are optimized for maximal coincidence rates with the temporal resolution of 100 ps.

We measure $g^{(2)}(0)$ for the idler conditioned on detecting a signal photon (a threefold coincidence measurement between the signal detector and both idler detectors), and also without any conditioning (a twofold coincidence measurement between the two idler detectors). We repeat this measurement for different signal-idler wavelength pairs connected by energy conservation (with collection bandwidth $\Delta\lambda = 0.9$ nm) [Fig. 2(a)] and for different $\Delta\lambda$ with $\lambda_s = 693$ nm and $\lambda_i = 795$ nm [Fig. 2(b)], showing that the conditional $g^{(2)}(0)$ is consistent for the different signal-idler wavelength pairs and bandwidths studied. It is important to note that shifting to a different signal-idler wavelength pair involves only moving the slits in front of the retroreflective mirrors (see Fig. 1) using micrometer stages, and does not require any optical realignment. We observe that the conditional $g^{(2)}(0)$ is far below the classical limit of unity at low pump power and increases for higher power, showing the increased emission probability for multiple photon pairs at higher pump power. {It should be noticed that at higher pump power, the approximation of $g^{(2)}(0) \approx [2p(2)/p^2(1)]$ in Eq. (3) may not be appropriate due to the increased probability of multiple-photon-pair process, such as the emission of

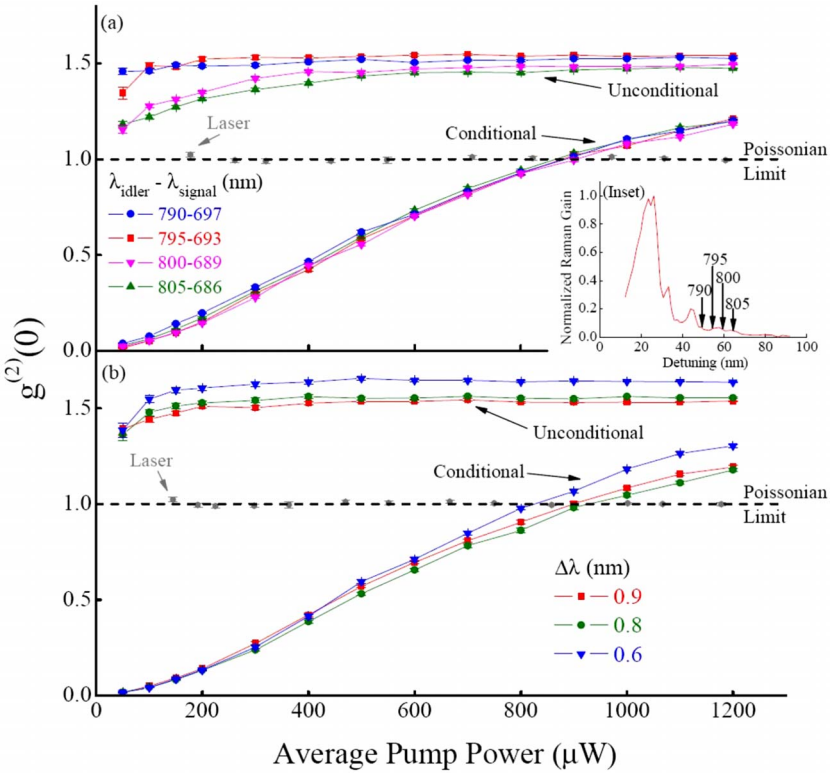

FIG. 2. (Color online) $g^{(2)}(0)$ for (a) various wavelengths at a bandwidth of $\Delta\lambda=0.9$ nm and (b) various bandwidths at signal (idler) wavelength of 693 (795) nm. Inset shows the measured Raman gain spectrum of the fiber. The lower sets of curves are heralded events and the upper sets are unheralded events. The classical, Poissonian, limit of 1 is shown as a dashed, black line. The scattered data points near the classical limit of 1 are measurements for the pulsed laser. For all points, error bars are one standard deviation and represent statistical errors. Lines are given only to guide the eye.

three photon pairs.} For comparison, we also measured $g^{(2)}(0)$ of the pulsed Ti:sapphire pump laser to be equal to the classical limit of 1 for all applied power levels, demonstrating that our pump laser approximates an ideal coherent laser source. Note that for the measurement of the pump laser, $g^{(2)}(0)$ is plotted versus pump powers that produce similar detected idler photon rates as the detected photon rates for the $g^{(2)}(0)$ measurement of the laser.

We list some of the values of conditional $g^{(2)}(0)$ versus the detected two-photon coincidence rate for a bandwidth of $\Delta\lambda=0.9$ nm in Table I. At 350 Hz detected coincidence rate, we have conditional $g^{(2)}(0)$ as low as 0.014, suppressed by a factor of more than 70 relative to the classical, Poissonian limit of 1. This detected pair rate corresponds to 50 μW average pump power (80 mW peak pump power) and, with our idler detection efficiency of 7%, a heralding efficiency (probability of emitting an idler photon from the end of the fiber given detection of a signal photon) of 0.51. As the coincidence rate is increased (by increasing the pump power), $g^{(2)}(0)$ increases due to the increased number of multiple-photon-pair events. At a detected coincidence rate of 12 kHz (peak pump power=490 mW, heralding efficiency $\approx$0.6) $g^{(2)}(0)\approx 0.3$. As demonstrated in Table I, for a given coincidence rate, $g^{(2)}(0)$ remains at the same level over a broad spectral range. For comparison, the best performing PDC source (also listed in Table I) exhibits $g^{(2)}(0)$ as low as 0.0014 at a bandwidth of $\Delta\lambda=6.9$ nm, a pump power (continuous wave) of 1.6 mW, a detection efficiency for the heralded photons in arm a (arm b) of 8.4% (9.6%), and heralding efficiency of 0.61 [12].

For the unheralded data shown in Fig. 2, we observe $g^{(2)}(0)$ to be slightly above 1, which is likely due to the presence of spontaneous Raman-scattered photons in the idler channel. We also observe $g^{(2)}(0)$ for unheralded events to be higher for idler wavelengths where the Raman scattering gain is higher (see inset of Fig. 2). For narrower collection bandwidths, the unheralded $g^{(2)}(0)$ increases, which is

TABLE I. Selected values of $g^{(2)}(0)$, detected signal-idler pair rates, and heralding efficiency (the probability of emitting an idler photon from the end of the fiber given detection of a signal photon) for different pump powers and signal-idler wavelengths and for the best performing PDC source. Uncertainties are one standard deviation and represent statistical errors.

λ_{signal} (nm)	λ_{idler} (nm)	$g^{(2)}(0)$	Detected pair rate (kHz)	Heralding efficiency
		Our source		
697	790	0.039 ± 0.003	0.28	0.47
		0.140 ± 0.004	2.91	0.53
		0.330 ± 0.008	11.9	0.60
693	795	0.014 ± 0.002	0.35	0.51
		0.095 ± 0.003	3.21	0.54
		0.300 ± 0.007	14.4	0.59
689	800	0.023 ± 0.002	0.33	0.51
		0.096 ± 0.003	3.24	0.57
		0.290 ± 0.007	12.7	0.63
686	805	0.029 ± 0.003	0.29	0.46
		0.110 ± 0.003	2.66	0.52
		0.310 ± 0.008	11.9	0.58
		PDC source [12]		
810	1550	0.0014 ± 0.0003	0.35	0.61

likely due to the smaller number of Raman scattered spectral modes entering the detection system. In this case, fewer spectral modes causes increase in $g^{(2)}(0)$ because the statistics of multimode light (in this case, multiple spectral modes) composed of many single modes each with thermal statistics approaches Poissonian statistics as the number of modes increases [20].

The relatively low single-photon detection efficiency in the current setup is mainly due to the inefficient free-space spectral filtering and spatial-mode mismatch between the microstructure fiber and the single-mode detection fiber. Thus, the efficiency can be improved by using spectral filters of higher transmittance and improving the spatial mode matching (for example, gradually tapering the end of the microstructure fiber to a bigger core size and then splicing it to a regular single-mode fiber). In addition, the use of photon-number-resolving detectors would allow us to obtain a more accurate measurement of multiphoton emission and to truly herald detection of a single signal photon.

In conclusion, we have demonstrated the reduction of multiple-photon-pair-emission probability by up to more than a factor of 70 compared to a Poissonian light source in a wavelength-tunable heralded single-photon source that uses four-wave mixing in a microstructure fiber. The strong suppression of multiple-photon-pair emission, combined with the wavelength tunability and single-spatial-mode output suggest that with further improvements in the photon collection efficiency, our source would be suitable for a variety of quantum-information applications.

This work has been supported in part by the Intelligence Advanced Research Projects Activity (IARPA) entangled photon source program, and the Multidisciplinary University Research Initiative Center for Photonic Quantum Information Systems (Army Research Office/DTO Program No. DAAD19-03-1-0199). E.A.G. acknowledges support from the Joint Quantum Institute. M.D.E. acknowledges support from the National Research Council.

[1] *The Physics of Quantum Information*, edited by D. Bouwmeester, A. Ekert, and A. Zeilinger (Springer, Berlin, 2000).
[2] L. Laflamme, E. Knill, and G. J. Milburn, Nature (London) **46**, 409 (2001).
[3] A. Beveratos, R. Brouri, T. Gacoin, A. Villing, J. P. Poizat, and P. Grangier, Phys. Rev. Lett. **89**, 187901 (2002).
[4] P. Michler *et al.*, Science **290**, 2282 (2000); C. Santori *et al.*, Nature (London) **419**, 594 (2002); V. Zwiller *et al.*, Appl. Phys. Lett. **82**, 1509 (2003); Z. Yuan *et al.*, Science **295**, 102 (2002); A. Kiraz, M. Atature, and A. Immamoglu, Phys. Rev. A **69**, 032305 (2004).
[5] J. Kim, O. Benson, H. Kan, and Y. Yamamoto, Science **397**, 500 (1999).
[6] F. De Martini, G. D. Giuseppe, and M. Marrocco, Phys. Rev. Lett. **76**, 900 (1996); C. Brunel, B. Lounis, P. Tamarat, and M. Orrit, *ibid.* **83**, 2722 (1999); B. Lounis and W. E. Moerner, Nature (London) **407**, 491 (2000).
[7] A. Kuhn, M. Hennrich, and G. Rempe, Phys. Rev. Lett. **89**, 067901 (2002); J. McKeever *et al.*, Science **303**, 1992 (2004).
[8] B. B. Blinov, D. L. Moehring, L.-M. Duan, and C. Monroe, Nature (London) **428**, 153 (2004); M. Keller, B. Lange, K. Hayasaka, W. Lange, and H. Walther, *ibid.* **431**, 1075 (2004).
[9] C. W. Chou, S. V. Polyakov, A. Kuzmich, and H. J. Kimble, Phys. Rev. Lett. **92**, 213601 (2004); T. Chanelière *et al.*, Nature (London) **438**, 833 (2005); M. D. Eisaman *et al.*, *ibid.* **438**, 837–841 (2005); J. Laurat *et al.*, Opt. Express **14**, 6912 (2006); D. N. Matsukevich, T. Chaneliere, S. D. Jenkins, S. Y. Lan, T. A. B. Kennedy, and A. Kuzmich, Phys. Rev. Lett. **97**, 013601 (2006); P. Kolchin, S. Du, C. Belthangady, G. Y. Yin, and S. E. Harris, *ibid.* **97**, 113602 (2006); J. K. Thompson *et al.*, Science **313**, 74 (2006); Z. S. Yuan, Y. A. Chen, S. Chen, B. Zhao, M. Koch, T. Strassel, Y. Zhao, G. J. Zhu, J. Schmiedmayer, and J.-W. Pan, Phys. Rev. Lett. **98**, 180503 (2007).
[10] C. Kurtsiefer, S. Mayer, P. Zarda, and H. Weinfurter, Phys. Rev. Lett. **85**, 290 (2000); A. Beveratos, R. Brouri, T. Gacoin, J.-P. Poizat, and P. Grangier, Phys. Rev. A **64**, 061802(R) (2001).
[11] C. K. Hong and L. Mandel, Phys. Rev. Lett. **56**, 58 (1986); A. B. U'Ren, C. Silberhorn, K. Banaszek, and I. A. Walmsley, *ibid.* **93**, 093601 (2004); S. Castelletto, I. P. Degiovanni, V. Schettini, and A. Migdall, Opt. Express **13**, 6709 (2005).
[12] S. Fasel *et al.*, New J. Phys. **6**, 163 (2004).
[13] A. B. U'Ren, C. Silberhorn, J. L. Ball, K. Banaszek, and I. A. Walmsley, Phys. Rev. A **72**, 021802(R) (2005).
[14] P. Grangier, G. Roger, and A. Aspect, Europhys. Lett. **1**, 173 (1986).
[15] A. Fedrizzi *et al.*, Opt. Express **15**, 15377 (2007).
[16] G. P. Agrawal, *Nonlinear Fiber Optics*, 2nd ed. (Academic Press, New York, 1995).
[17] J. Fan and A. Migdall, Opt. Express **15**, 2915 (2007); J. Fan, M. D. Eisaman, and A. Migdall, Phys. Rev. A **76**, 043836 (2007); Opt. Express **15**, 18339 (2007).
[18] J. Fulconis, O. Alibart, J. L. O'Brien, W. J. Wadsworth, and J. G. Rarity, Phys. Rev. Lett. **99**, 120501 (2007).
[19] R. J. Glauber, Phys. Rev. **130**, 2529 (1963); **131**, 2766 (1963).
[20] R. Loudon, *The Quantum Theory of Light*, 3rd ed. (Oxford University Press, Oxford, 2000).
[21] S. J. Kuo, D. T. Smithey, and M. G. Raymer, Phys. Rev. A **43**, 4083 (1991).
[22] S. V. Polyakov, A. Migdall, and S. W. Nam (unpublished).